Fizika Nizkikh Temperatur, 2003, v. 29, No. 8, p. 885–888

Magnetic and transport properties of $La_{0.8}Sr_{0.2}MnO_3/La_{0.8}Ca_{0.2}MnO_3$ bilayer

V.G. Prokhorov, G.G. Kaminsky, and V.A. Komashko

Institute of Metal Physics of the National Academy of Sciences of Ukraine, 36 Vernadsky bul'var, Kiev, 03142, Ukraine
E-mail: pvg@imp.kiev.ua

Y.P. Lee and J.S. Park

Quantum Photonic Science Research Center and Department of Physics, Hanyang University, Seoul, 133–791 Korea

Received January 21, 2003

The effects of lattice strain on the magnetic and the transport properties of $La_{0.8}Sr_{0.2}MnO_3$ films grown on an (001) $LaAlO_3$ substrate and on a $La_{0.8}Ca_{0.2}MnO_3$ layer were studied. It was observed that the metal-insulator and the ferromagnetic transitions occur at higher temperatures for the film deposited on $La_{0.8}Ca_{0.2}MnO_3$ layer than on $LaAlO_3$. The dependence of Curie temperature on the bulk and the Jahn–Teller strains were also determined.

PACS: **71.30.+h**, **75.70.–i**

Doped colossal-magnetoresistance (CMR) manganite perovskites exhibit a strong correlation between their lattice structure and magneto-transport properties [1]. This phenomenon becomes apparent in thin films. The lattice strain (and stress) accumulated during epitaxial growth of a film plays an important role in the formation of the spin- and the charge-ordered states, the metal-insulator transition temperature, and the value of magnetoresistance [2–4].

The effect of the kind of single-crystal substrate on the magnetic and the electronic properties of manganite films has been investigated well [5,6]. On the other hand, to develop hybrid devices based on multilayered CMR films detailed information on the mutual influence between constituent layers is required. It is expected that the magnetic and the transport properties of a multilayer structure can substantially differ from those of the individual films of the constituent layers. In this work we report experimental results for $La_{0.8}Sr_{0.2}MnO_3$ (LSM) and $La_{0.8}Ca_{0.2}MnO_3$ (LCM) films and for a $La_{0.8}Sr_{0.2}MnO_3/La_{0.8}Ca_{0.2}MnO_3$ bilayer (BL).

All films were prepared by rf magnetron sputtering using a so-called «soft» (or powder) target [7]. The total pressure in the chamber was $5 \cdot 10^{-2}$ Torr with a 3:1 $Ar–O_2$ gas mixture. The substrate was a $LaAlO_3$ (001) single crystal (LAO) with an out-of-plane lattice parameter $c \simeq 0.379$ nm for pseudocubic symmetry. The substrate temperature during deposition was 750°C. Both LSM and LCM films were deposited with a thickness $d \simeq 60$ nm, and the BL was deposited with the same thickness for each layer and with LSM on top. The θ–2θ x-ray diffraction (XRD) patterns were obtained using a Rigaku diffractometer and CuK_α radiation. The lattice parameters evaluated directly from the XRD data were plotted against $\cos^2\theta/\sin\theta$. A more precise determination of the lattice parameter was obtained extrapolating a straight line to $\cos^2\theta/\sin\theta = 0$. The resistance measurements were carried out using the four-probe method in the temperature range of 4.2–300 K and a magnetic fields up to 5 T. The magnetization in a field up to 100 Oe and the susceptibility at 500 Hz were obtained with a Quantum Design SQUID magnetometer in the temperature range of 4.2–300 K.

Figure 1,*a* presents the θ–2θ XRD scans for LSM (curve *1*), LCM (curve *2*) and BL (curve *3*) films. The high intensities of the (00*l*) peaks show that the deposition results in highly *c*-oriented films. Figure 1,*b* shows that the location of the (002) Bragg peak for the BL is almost coincident with that for the LCM film. In contrast, the peak for the LSM film is dis-

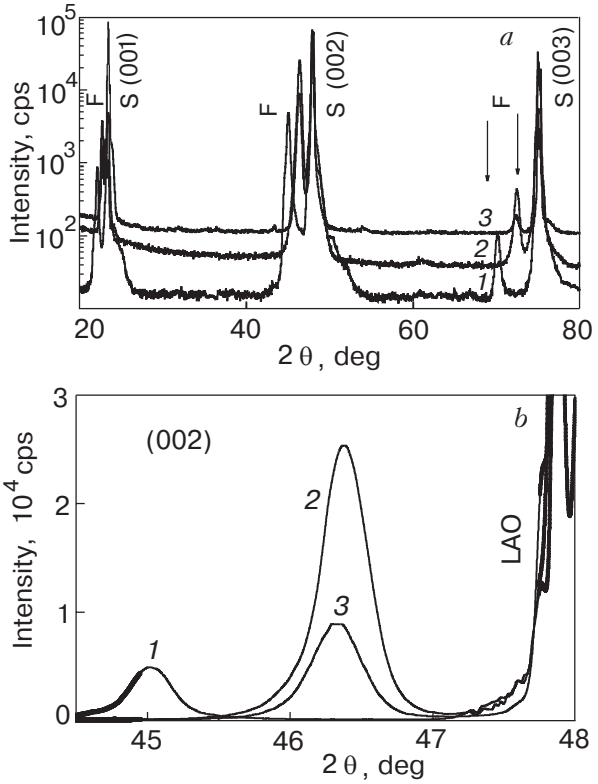

Fig. 1. θ–2θ XRD patterns of LSM (*1*), LCM (*2*) and BL (*3*) films (*a*). The (002) XRD peaks (*b*).

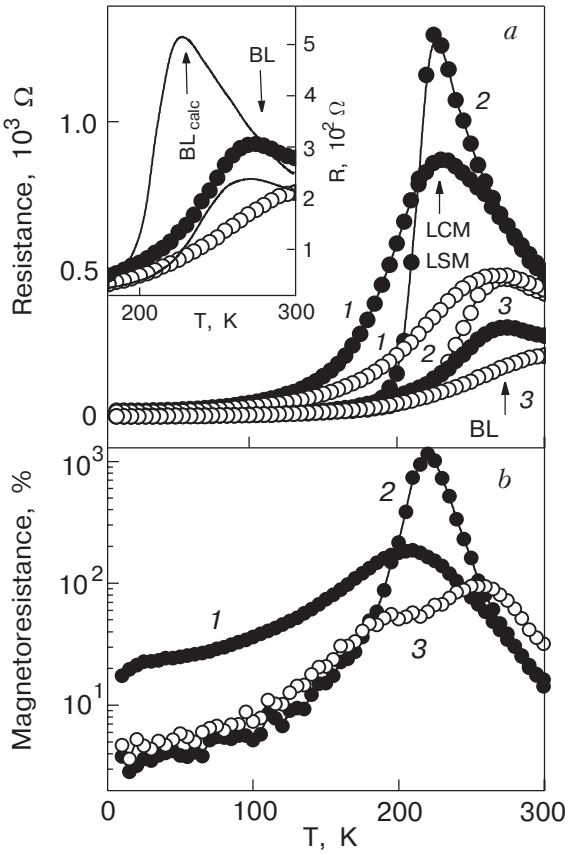

Fig. 2. Temperature dependence of the resistance for LSM (*1*), LCM (*2*) and BL (*3*) films without (filled circles) and with (open circles) an applied magnetic field of 5 T. The lines are visual aids. Inset: The experimental (circles) and computed (solid line) dependences $R(T)$ for the BL film. The arrows show the MI transition temperatures for different samples (*a*). Temperature dependence of the magnetoresistance for LSM (*1*), LCM (*2*) and BL (*3*) films. The lines are visual aids (*b*).

tinctly shifted to a smaller angle. Therefore the analysis of XRD data reveals that the out-of-plane lattice parameter for the LSM film is strongly dependent on the substrate: $c \simeq 0.398$ nm on the LAO substrate and $c \simeq 0.391$ nm on the $La_{0.8}Ca_{0.2}MnO_3$ film with lattice parameter $c \simeq 0.3905$ nm.

Figure 2,*a* displays the temperature dependence of the resistance R for LSM (curve *1*), LCM (curve *2*) and BL (curve *3*) films without (filled circles) and with (open circles) an applied magnetic field of 5 T. The magnetic field was directed at right angle to both the film surface and the transport current. The experimental curves show that the metal–insulator (MI) transition temperatures for both LSM and LCM films are very close, about 230 K. The BL film undergoes a MI transition at 280 K, which is higher than for the individual films. The MI transition temperatures for all samples are indicated by arrows. The inset in Fig. 2,*a* shows that the $R(T)$ behavior of the BL film differs from that predicted by the simple two parallel-resistor model (solid line), where the first resistor corresponds to the LSM film (curve *1*) and the second one to the LCM film (curve *2*). Since the lattice parameter c changes significantly only for the LSM film deposited on the LCM layer, it is reasonable to inter that the increase in the MI transition temperature for BL is due to the improved magnetic and electronic properties of the LSM film only.

Figure 2,*b* presents the temperature-dependent magnetoresistance, $\mathrm{MR}(\%) = [R(0) - R(H)]100/R(H)$, obtained for LSM (curve *1*), LCM (curve *2*) and BL (curve *3*) film in an applied magnetic field of 5 T. Here, $R(0)$ and $R(H)$ are the resistances without and with a magnetic field. It is seen that a slight enhancement in the MR for BL, with respect to the individual LSM and LCM films, is observed only at high temperatures. In the low-temperature range the MR of BL remains smaller than that of the LSM film and mimics the $\mathrm{MR}(T)$ behavior for the LCM film.

Figure 3,*a* shows both field-cooled (FC) and zero-field-cooled (ZFC) temperature-dependent magnetization curves for LSM (curve *1*), LCM (curve *2*) and BL (curve *3*) films. The arrows show the corresponding Curie temperatures. The LCM film mani-

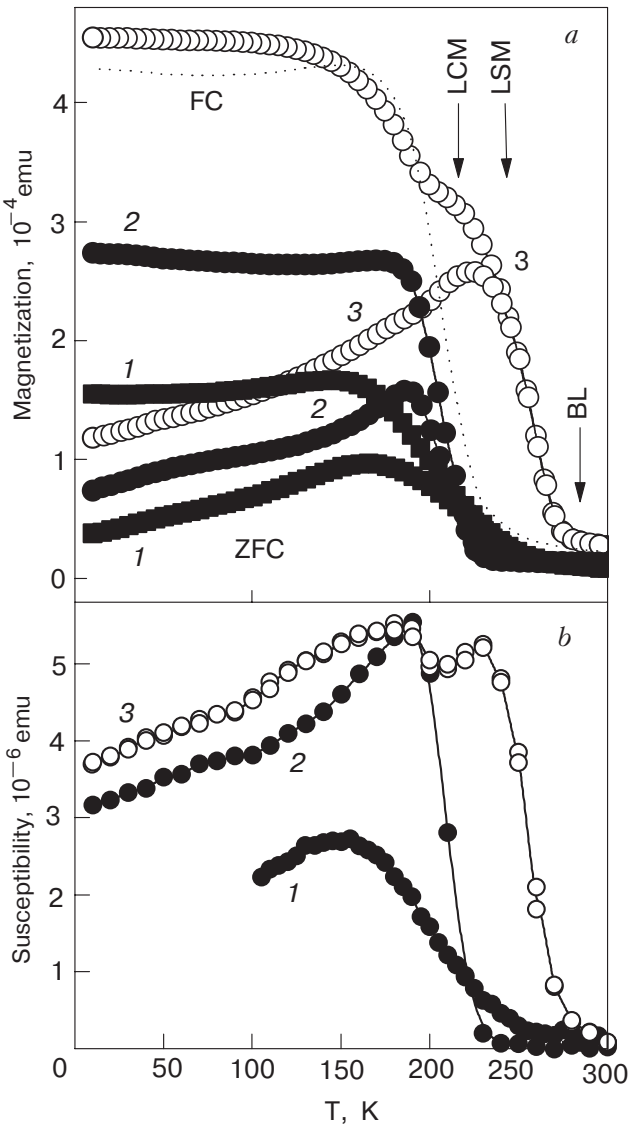

Fig. 3. Temperature dependence of the FC and the ZFC magnetization for LSM (*1*), LCM (*2*) and BL (*3*) films. The lines are visual aids. The arrows indicate the magnetic transition temperatures for different samples. The dashed line was obtained by simple addition of the FC $M(T)$ curves (*1*) and (*2*) (*a*). Temperature dependence of the susceptibility for LSM (*1*), LCM (*2*) and BL (*3*) films. The lines are visual aids (*b*).

fests a sharp transition to the ferromagnetic state at $T_C = 230$ K, in agreement with the published results for as-grown films [3]. In contrast, the LSM film displays a broad and smooth magnetic transition near $T_C \simeq 260$ K. Moreover, the absolute value of the saturated FC magnetization is half of that for the LCM film of similar thickness. The same behavior of $M(T)$ and a lower value of T_C with respect to the bulk value have been observed previously for a $La_{0.67}Sr_{0.33}MnO_3$ film deposited on a LAO substrate [8,9]. It was explained by the 3-dimensional strain states in the film, governed by the epitaxial mode of film growth. The temperature-dependent magnetization for BL is significantly different from that predicted by simply adding the $M(T)$ values for both individual LSM and LCM films. The dashed line in Fig. 3,*a* shows the predicted curve: $M_{BL}(T) = M_{LCM}(T) + M_{LSM}(T)$, where $M_{LCM}(T)$ and $M_{LSM}(T)$ are the magnetizations for the LCM and the LSM films, respectively. Since the thicknesses of the individual films are similar to those of the corresponding layers in BL, the added curve fits the experimental data fourty well at low temperatures (in the saturation magnetization range). However, the ferromagnetic transition of the BL film occurs at a higher temperature ($T_C \simeq 280$ K) than predicted. This result confirms that a significant change occurs in the magnetic properties of the LSM film deposited on LCM with respect to that on LAO.

This conclusion is supported by the temperature dependences of susceptibility for LSM (curve *1*), LCM (curve *2*) and BL (curve *3*) films in Fig. 3,*b*. Since the low-temperature susceptibility peak for BL (curve *3*) mimics that of the individual LCM film, it can be concluded that the second peak belongs to the LSM layer in the BL. It is evident that the magnetic transition of the LSM film deposited on LCM becomes sharper and the saturated magnetization is achieved at a higher temperature than for a bare LSM film (see curve *1*).

Let us consider the possible mechanisms of enhanced magnetic and transport properties of the LSM film on LCM with respect to that on LAO. The aforementioned analysis of x-ray data showed that the out-of-plane lattice parameter c is larger for LSM/LAO. It is well known that LSM thin films grown on LAO substrates exhibit an out-of-plane uniaxial tensile strain and, correspondingly, an in-plane biaxial compression [9,10]. Assuming that the film is strained from the ideal bulk structure and that the structure is a single perovskite, the in-plane lattice parameter of film can be estimated from the unit cell volume in the bulk. The bulk $La_{0.8}Sr_{0.2}MnO_3$ compound has a rhombohedral pseudocubic symmetry ($R\bar{3}c$) with hexagonal lattice parameters of $a_h \simeq 0.5517$ nm and $c_h \simeq 1.3359$ nm [11]. They are equivalent to cubic lattice parameters of $a \simeq b \simeq c \simeq 0.3871$ nm and to unit cell volume $V \simeq 0.058$ nm^3. Therefore, the in-plane lattice parameter for our LSM/LAO is $\sqrt{V}/c \simeq a \simeq$ $\simeq 0.3828$ nm, which is almost identical to the value obtained for an epitaxial $La_{0.67}Sr_{0.33}MnO_3$ thin film [1]. For our LSM/LCM the in-plane lattice parameter is larger and equals $a \simeq 0.3852$ nm. This difference between film and bulk lattice parameters leads to the formation of the above-mentioned in-plane biaxial

compressive strain, $\varepsilon_{100} = (a_{\text{film}} - a_{\text{bulk}})/a_{\text{bulk}}$, and the out-of-plane uniaxial tensile strain, $\varepsilon_{001} = (c_{\text{film}} - c_{\text{bulk}})/c_{\text{bulk}}$. The calculations performed show that $\varepsilon_{100} \simeq -1.37\%$ and $\varepsilon_{001} \simeq 2.8\ \%$ for the LSM/LAO and -0.49% and 1%, respectively, for the LSM/LCM. For weaker strains and cubic symmetry the Curie point can be expressed as, according to Millis model [12],

$$T_C(\varepsilon) = T_C(\varepsilon = 0)\left(1 - \alpha\varepsilon_B - \frac{1}{2}\Delta\,\varepsilon_{JT}^2\right),$$

where $\varepsilon_B = (2\varepsilon_{100} + \varepsilon_{001})$ is the bulk strain, $\varepsilon_{JT} = \sqrt{2/3}\,(\varepsilon_{001} - \varepsilon_{100})$ is the Jahn–Teller strain, $\alpha = (1/T_C)(dT_C/d\varepsilon_B)$, and $\Delta = (1/T_C)(d^2T_C/d\varepsilon_{JT}^2)$. For the last two quantities we are took the values from Ref. 12, i.e. $\alpha = 10$ and $\Delta = 1000$. Using this equation and the values obtained for ε_{100} and ε_{001} in our LSM film and layer we calculated the change in Curie temperature $T_{C_{\text{LSM/LCM}}}^{\text{calc}}/T_{C_{\text{LSM/LAO}}}^{\text{calc}} \simeq 1.07$, which is an excellent agreement with our experimental result $T_{C_{\text{LSM/LCM}}}/T_{C_{\text{LSM/LAO}}} \simeq 1.077$. This confirms the strong correlation between crystal lattice distortion and the electronic and magnetic states in CMR materials.

In summary, the magnetic and the transport properties of $La_{0.8}Sr_{0.2}MnO_3$ films grown on an (001) $LaAlO_3$ substrate and on a $La_{0.8}Ca_{0.2}MnO_3$ layer were studied. It was shown that the metal-insulator and the ferromagnetic transitions occur at higher temperatures for the film deposited on $La_{0.8}Ca_{0.2}MnO_3$ layer than on $LaAlO_3$. The enhanced magnetoresistance and ferromagnetic ordering in the $La_{0.8}Sr_{0.2}MnO_3/La_{0.8}Ca_{0.2}MnO_3$ bilayer can be explained by lattice strain relaxation in the $La_{0.8}Sr_{0.2}MnO_3$ film.

This work was funded by the KOSEF through the Quantum Photonic Science Research Center.

1. F. Tsui, M.C. Smoak, T.K. Nath, and C. B. Eom, *Appl. Phys. Lett*. **76**, 2421 (2000).
2. R.A. Rao, D. Lavric, T.K. Nath, C.B. Eom, L. Wu, and F. Tsui, *Appl. Phys. Lett*. **73**, 3294 (1998).
3. S. Jacob, T. Roch, F.S. Razavi, G.M. Gross, and H.-U. Habermeier, *J. Appl. Phys*. **91**, 2232 (2002).
4. A. Biswas, M. Rajeswari, R.C. Srivastava, T. Venkatesan, R.L. Green, Q. Lu, A.L. de Lozanne, and A.J. Millis, *Phys. Rev*. **B63**, 184424 (2001).
5. O.I. Lebedev, G. Van Tendeloo, S. Amelinckx, H.L. Ju, and K.M. Krishnan, *Philos. Mag*. **80**, 673 (2000).
6. J.R. Sun, C.F. Yeung, K. Zhou, L.Z. Zhou, C.H. Leung, H.K. Wong, and B.G. Shen, *Appl. Phys. Lett*. **76**, 1164 (2000).
7. V.G. Prokhorov, G.G. Kaminsky, V.A. Komashko, J.S. Park, and Y.P. Lee, *J. Appl. Phys*. **90**, 1055 (2001).
8. T.K. Nath, R.A. Rao, D. Lavric, C.B. Eom, L. Wu, and F. Tsui, *Appl. Phys. Lett*. **74**, 1615 (1999).
9. A.M. Haghiri-Gosnet, J. Wolfman, B. Mercey, Ch. Simon, P. Lecoeur, M. Korzenski, M. Hervieu, R. Desfeux, and G. Baldinozzi, *J. Appl. Phys*. **88**, 4257 (2000).
10. Y.H. Li, K.A. Thomas, P.S.I.P.N. de Silva, L.F. Cohen, A. Goyal, M. Rajeswari, N.D. Mathur, M.G. Blamire, J.E. Evetts, T. Venkatesan, and J.L. MacManus-Driscoll, *J. Mater. Res*. **13**, 2161 (1998).
11. J.F. Mitchell, D.N. Argyriou, C.D. Potter, D.G. Hinks, J.D. Jorgensen, and S.D. Bader, *Phys. Rev*. **B54**, 6172 (1996).
12. A.J. Millis, T. Darling, and A. Migliori, *J. Appl. Phys*. **83**, 1588 (1998).